JOURNAL OF MATERIALS SCIENCE **38** (2003) 2767–2770

Perovskite formation and dielectric responses in $Pb(Zn_{1/3}Nb_{2/3})O_3$-modified $Pb(Zn_{1/3}Ta_{2/3})O_3$-$PbTiO_3$ ceramics

D.-H. SUH, N.-K. KIM
Department of Inorganic Materials Engineering, Kyungpook National University, Daegu 702-701, Korea
E-mail: nkkim@knu.ac.kr

$Pb(Zn_{1/3}Ta_{2/3})O_3$-$PbTiO_3$ ceramic compositions were modified by the introduction of Nb to the octahedral lattice sites. Resultant tendencies in the perovskite formation and dielectric properties were examined. System powders were prepared using a B-site precursor method. Developed structures and lattice parameters of the system compositions were investigated by powder X-ray diffractometry, from which the parameter of a hypothetical perovskite $Pb(Zn_{1/3}Ta_{2/3})O_3$ is proposed. Weak-field low-frequency dielectric responses of the system ceramics were measured.

1. Introduction

$Pb(Zn_{1/3}Nb_{2/3})O_3$ (PZN) is a well-known relaxor-ferroelectric compound [1, 2] with a dielectric maximum temperature of 140°C (single crystal [1, 3]). PZN of a perovskite structure has been prepared only under very high pressures [4, 5] or via mechanochemical reaction routes [6], but not by conventional mixed-oxide processes. Unlike PZN, however, perovskite $Pb(Zn_{1/3}Ta_{2/3})O_3$ (PZT, which in the present paper does not stand for $Pb(Zr,Ti)O_3$) has not yet been synthesized by any process [7, 8]. The difficulties can be more or less attributed to the less-ionic nature of Ta, as compared with that of Nb [9]. Meanwhile, $PbTiO_3$ (PT) is a normal-ferroelectric perovskite with a Curie temperature of 490°C. The temperature-dependent dielectric constant spectrum of PT is quite sharp, whereas those of the ferroelectric relaxors are rather diffuse.

In a $(1-x)$PZT-xPT binary system [10], only a pyrochlore structure formed at $x \leq 0.2$. However, perovskite started to develop at PT fractions as low as 0.3. Although perovskite formation was not realized at low values of x, replacement of the octahedral cations of Ta by Nb (with a higher ionicity value [9]) might promote perovskite development. In this regard, PZN introduction (20 mol%) into the PZT-PT system was attempted in the present study, hoping that the perovskite formation (especially at PZT-rich compositions) could be enhanced. In order to suppress the formation of harmful pyrochlore(s), system powders were synthesized using a B-site precursor method [11, 12], which is essentially identical to (but conceptually more comprehensive than) the columbite process [13, 14]. Effectiveness of the methods in increasing the perovskite phase yields can be found in many works [13–17].

2. Experimental

Nominal compositions of the 20 mol% PZN-substituted PZT-PT system can be written as $(0.8-x)$PZT-0.2PZN-xPT, i.e., $Pb[(Zn_{1/3}Ta_{2/3})_{0.8-x}(Zn_{1/3}Nb_{2/3})_{0.2}Ti_x]O_3$. The values of x were changed at regular intervals of 0.2 in the 0.0–0.8 range. The expressions of $Pb(Zn_{1/3}Ta_{2/3})O_3$ (PZT) in the present paper simply indicate the stoichiometric composition and do not necessarily imply the perovskite formation. B-site precursor system powders of $[(Zn_{1/3}Ta_{2/3})_{0.8-x}(Zn_{1/3}Nb_{2/3})_{0.2}Ti_x]O_2$ (i.e., $[Zn_{(1.0-x)/3}Ti_xTa_{(1.6-2x)/3}Nb_{0.4/3}]O_2$) were prepared from the high purity (>99.5%) oxide chemicals after calcination at 1050–1150°C for 2 h in air. The precursor powders were mixed with PbO in stoichiometric proportions (i.e., without any addition of excess amounts) and were calcined at 800–850 and 800–1050°C for 2 h each for enhancing the perovskite formation, with intermediate milling stages. Calcined powders were examined by X-ray diffraction (XRD) in order to identify the phases formed. The powders were formed into pellets and fired for 1 h at 1100–1250°C in a multiple-enclosure crucible setup (with identical composition powders surrounding the pellets [18]) to maintain the powder compositions as closely to the nominal values as possible. Major faces of the sintered pellets were Au-sputtered and Ag-overcoated for electrical contact. Weak-field ($\sim 1\ V_{rms}$/mm) low-frequency (1, 10, 100, and 1000 kHz) dielectric constant values of the system ceramics were measured using an impedance analyzer.

3. Results and discussion

XRD patterns of the B-site precursor system $[(Zn_{1/3}Ta_{2/3})_{0.8-x}(Zn_{1/3}Nb_{2/3})_{0.2}Ti_x]O_2$ are displayed in Fig. 1. The pattern of $x = 0.0$ (i.e., $[(Zn_{1/3}Ta_{2/3})_{0.8}$-

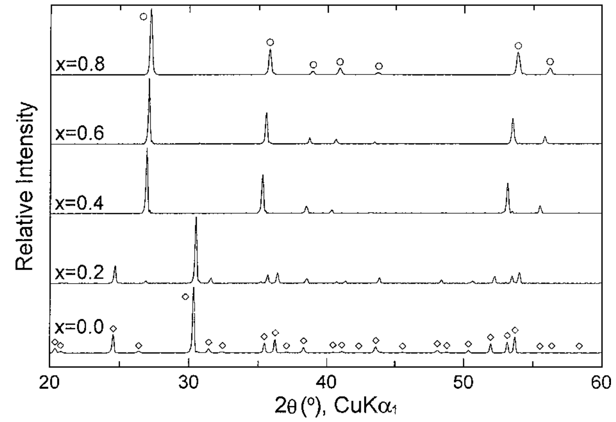

Figure 1 Developed structures in the $[Zn_{1/3}Ta_{2/3})_{0.8-x}(Zn_{1/3}Nb_{2/3})_{0.2}$-$Ti_x]O_2$ B-site precursor system. (◇) tri-αPbO_2, (○) rutile.

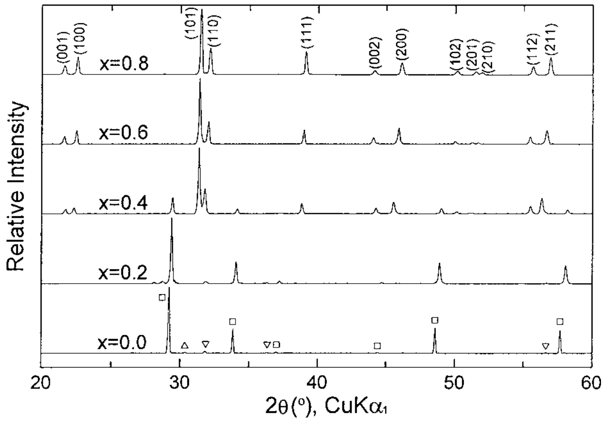

Figure 2 Developed structures in the $(0.8-x)$PZT-0.2PZN-xPT system. (□) pyrochlore, (△) PbO, (▽) ZnO, (hkl) perovskite.

$(Zn_{1/3}Nb_{2/3})_{0.2}]O_2$) matched exactly to that of the tri-αPbO_2 structure ($ZnTa_2O_6$, ICDD #39-1484), indicating that the 20% component of $(Zn_{1/3}Nb_{2/3})O_2$ (columbite structure, ICDD #37-1371) had been completely dissolved into the host structure of tri-αPbO_2. Nevertheless, angular shifts due to unit cell expansion/contraction by the introduction of foreign octahedral cations could not be observed, as the size of Nb^{5+} is identical to that of Ta^{5+}: 0.064 nm [19]. In contrast, only a rutile structure was identified at $x = 0.4$–0.8. By careful examination of the diffraction angles, however, the rutile was neither of TiO_2 (ICDD #21-1276) nor of $[(Zn_{1/3}Nb_{2/3})_{1/2}Ti_{1/2}]O_2$ (ICDD #39-291) or $[(Zn_{1/3}Ta_{2/3})_{1/2}Ti_{1/2}]O_2$ (ICDD #39-292). Rather, it was a solid solution formed thereof. The composition of $[(Zn_{1/3}Nb_{2/3})_{0.2}Ti_{0.8}]O_2$ ($x = 0.8$), for instance, could be resolved as $0.4[(Zn_{1/3}Nb_{2/3})_{1/2}Ti_{1/2}]O_2 + 0.6TiO_2$ (ZNT + T). A diffiraction angle of say 56.2° (the last peak at $x = 0.8$) can be readily obtained by applying the theoretical ratio of ZNT:T = 4:6 (by mole) to the corresponding values of 55.6° and 56.6°. Meanwhile, the spectrum of $x = 0.2$ (i.e., $[(Zn_{1/3}Ta_{2/3})_{0.6}(Zn_{1/3}Nb_{2/3})_{0.2}Ti_{0.2}]O_2$) was mostly of the tri-$\alpha PbO_2$ structure, along with a small fraction of the rutile solid solution, indicating that most of the $(Zn_{1/3}Nb_{2/3})O_2$ and TiO_2 of 20 mol% each had been again almost dissolved into the host structure. The diffraction angles in the whole system increased in general with increasing values of x, which will be discussed later.

Developed structures in the $(0.8 - x)$PZT-0.2PZN-xPT system were examined using the atmosphere powders (used during the sintering stage) and the results are presented in Fig. 2. The spectra of $x = 0.0$ and 0.2 were identified to be that of the cubic pyrochlore. It is not easy, however, to describe the pyrochlore composition, as there are many varieties (with similar diffraction patterns) formable at the PZT-rich region in the PbO-ZnO-$(Ta/Nb)_2O_5$-TiO_2 system: namely, $Pb_{1.83}Zn_{0.29}Ta_{1.71}O_{6.39}$ (ICDD #34-395), $Pb_3Ta_4O_{13}$ (ICDD #17-613), $Pb_4Ta_6O_{19}$ (ICDD #36-1096), $Pb_3Ta_2TiO_{10}$ (ICDD #17-610), $Pb_3Ta_4TiO_{15}$ (ICDD #24-590), and so on. At present, the pyrochlore seems to be solid solutions developed thereof. The components of PZN ($x = 0.0$ and 0.2) and PT ($x = 0.2$) of 20 mol% each seem to have been dissolved totally into the pyrochlore solid solution. When pyrochlore(s) formed from powder mixtures of the perovskite stoichiometry, however, certain fractions of PbO and ZnO would remain, the presence of which were actually confirmed: PbO (△) and ZnO (▽). At $x = 0.4$, the perovskite structure started to develop suddenly and became the sole phase present at $x = 0.6$ and 0.8. (hkl) indices of the perovskite structure (based on a tetragonal symmetry) are placed to all diffraction peaks of $x = 0.8$. It is interesting to note that the composition (where perovskite first appeared) coincides with the composition, where the tri-αPbO_2 structure disappeared, Fig. 1. The observation can be understood by considering that a pyrochlore structure (which is less ionic in character, as compared to the perovskite) would result, when the $ZnTa_2O_6$ component of a tri-αPbO_2 structure is reacted with PbO. Furthermore, extraneous reflections (associated with the perovskite superlattice) could not be detected at all, indicating that any compositional ordering among the four octahedral cation species had not developed in the macroscopic scale.

Perovskite phase yields of the system compositions, determined by intensity comparison between the perovskite {110} and pyrochlore (222) reflections, are plotted in Fig. 3. As the {110} peaks of the perovskite structure are split, integrated intensities were used in the

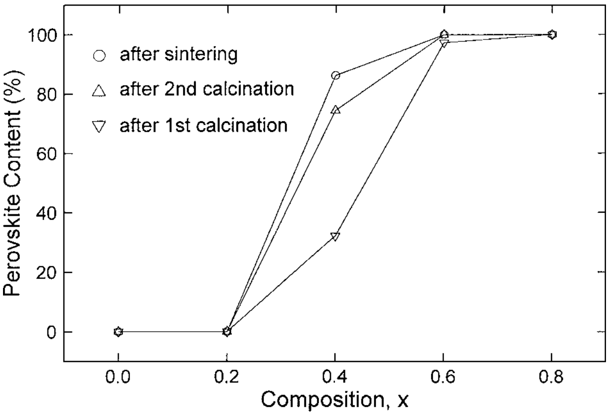

Figure 3 Perovskite content of the system compositions, after each heat-treatment stage.

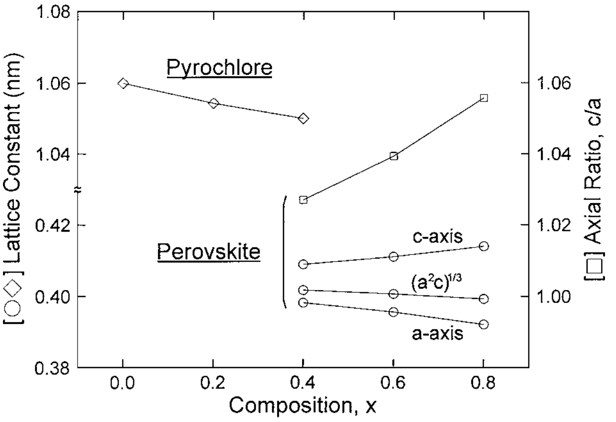

Figure 4 Dependencies of the pyrochlore/perovskite lattice parameters and perovskite axial ratios upon compositional change.

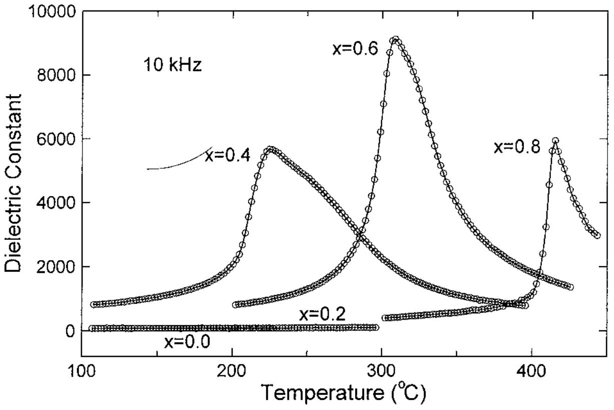

Figure 5 Dielectric constant spectra of the system ceramics.

calculation. The perovskite yields at $x = 0.0$ and 0.2 are 0% (even after sintering), as only the pyrochlore structure was present, Fig. 2. The content then abruptly increased to 86% ($x = 0.4$, after sintering) and 100% ($x = 0.6$ and 0.8) at the expense of the pyrochlore. The perovskite yield also increased with the heat-treatment stages: e.g., for $x = 0.4$, the values were 32%, 74%, and 86% after the first and second calcinations, and after sintering.

Lattice parameters of the pyrochlore/perovskite structures and axial ratios (or tetragonality factors, "c/a") are plotted in Fig. 4 with compositional changes. The pyrochlore parameters decreased linearly from 1.0599 nm ($x = 0.0$) to 1.0499 nm ($x = 0.4$). The value of 1.0599 nm is identical to that, interpolated from 1.0598 nm in $Pb_{1.83}Zn_{0.29}Ta_{1.71}O_{6.39}$ (ICDD #34-395) and 1.0602 nm in $Pb_{1.83}Zn_{0.29}Nb_{1.71}O_{6.39}$ (ICDD #34-374). As for the perovskite structure, in contrast, the lattice parameter "a" decreased slightly from 0.3982 nm ($x = 0.4$) to 0.3921 nm ($x = 0.8$), whereas "c" increased at similar rates from 0.4089 nm to 0.4140 nm at the same composition interval. Consequently, the axial ratio of 1.027 at $x = 0.4$ increased rapidly to 1.056 at $x = 0.8$, reflecting the gradual peak splittings in the identical $\{hkl\}$ families with increasing x (Fig. 2). Nontheless, the average lattice parameter "$(a^2c)^{1/3}$" decreased steadily from 0.4017 nm ($x = 0.4$) to 0.3993 nm ($x = 0.8$). The continuous decreases in the pyrochlore/perovskite lattice parameters, reflected in the overall shifts of the diffraction peaks to higher angles with increasing x (Fig. 2), can be well explained by the gradual replacement of small-sized Ti ($r = 0.0605$ nm [19]) for $Zn_{1/3}Ta_{2/3}$ ($r = 0.0673$ nm [19]: weighted-average value). It is interesting to note, however, that the variations of the lattice parameter of the pyrochlore structure is steeper (as compared with that of the perovskite), which seems to be related to the structurally more-open (i.e., less-dense and consequently more easily-compressible) nature of the pyrochlore (e.g., 7.349 g/cm^3 ($Pb_{1.83}Zn_{0.29}Nb_{1.71}O_{6.39}$, ICDD #34-374) vs. 8.376 g/cm^3 ($Pb(Zn_{1/3}Nb_{2/3})O_3$, ICDD #22-662)). Meanwhile, the lattice parameter quotient of $a_{pyro.}/a_{perov.}$ was 2.61 ($x = 0.4$), which falls within the reported range of 2.61–2.64 in various Pb-based compositions [8, 16, 20, 21].

By assuming a linear relationship in the lattice parameter changes, that of a hypothetical perovskite PZT was 0.4037 nm, as extrapolated from 0.4062 nm (PZN, ICDD #22-662) and 0.4042 nm (extrapolated from the "$(a^2c)^{1/3}$" values at $x = 0.4$–0.8 down to $x = 0.0$, i.e., 0.8PZT-0.2PZN). So far, three different extrapolated values of 0.4007 nm [21], 0.4012 nm [21], and 0.4050 nm [22] have been proposed as the lattice parameter of PZT. Among the four (three previous values plus present one), however, that of 0.4037 nm (obtaied in the present study) seems to be closest to the intrinsic value. This is because the present value was obtained by extrapolation at the shortest composition interval. Meanwhile, from the values of 0.4062 nm of PZN (ICDD #22-662) and 0.3982 nm (weighted-average value) of PT (ICDD #6-452), an interpolated value of 0.3998 nm could be obtained for 0.2PZN-0.8PT ($x = 0.8$), which is quite close to the observed value of 0.3993 nm.

Dielectric constant spectra of the system ceramics are compared in Fig. 5. The spectra of $x = 0.0$ and 0.2 (where perovskite phase yield = 0%) did not show any maximum. Instead, the dielectric constants merely decreased with increasing temperature, with room-temperature values of 79 ($x = 0.0$) and 86 ($x = 0.2$). Then, the dielectric constant peak of 5700 developed ($x = 0.4$) and increased to 9100 ($x = 0.6$), followed by a decrease to 5900 ($x = 0.8$). The spectra of $x = 0.4$ and 0.6, however, exhibited unusual features of a second hump at the paraelectric temperature range, the underlying mechanism of which needs to be investigated further. As for the frequency dependence, little dispersion in the dielectric constant spectra was observed with negligible increases in the dielectric maximum temperatures (<1°C, $x = 0.4$–0.8), as the measurement frequency changed from 1 kHz to 1 MHz. The dielectric maximum temperatures, however, increased quite substantially with the compositional change: 225°C ($x = 0.4$) to 415°C ($x = 0.8$).

4. Summary

In the B-site precursor system, only tri-αPbO_2 and rutile structures were detected at $x = 0.0$ and $x = 0.4$–0.8, respectively, with the two structures coexisting at $x = 0.2$. After the addition of PbO and calcination, pyrochlore (along with negligible amounts of PbO and

ZnO) was the sole structure developed at PZT-rich compositions of $x = 0.0$ and 0.2, whereas only a perovskite structure of a tetragonal symmetry was identified at $x = 0.6$ and 0.8. The perovskite formation yields increased with increasing PT concentration. At the same time, (average) lattice parameters of the pyrochlore and perovskite structures decreased systematiclly by the influence of the small-sized Ti ions gradually occupying the octahedral lattice sites, whereas the axial ratio of the tetragonal perovskite increased rapidly. A lattice parameter of the hypothetical perovskite PZT was proposed to be 0.4037 nm. In the dielectric constant measurements, the maximum peaks were observable only at $x = 0.4$, 0.6, and 0.8. The phase transition modes of the first two compositions were rather diffuse, whilst that of the last one was quite sharp. With respect to the frequency change (1 kHz → 1 MHz), the dielectric maximum temperature increased only negligibly, $<1^\circ$C.

Acknowledgment

This work was supported by a grant from the Korea Science and Engineering Foundation, Basic Research Program (R02-2000-00239).

References

1. V. A. BOKOV and I. E. MYL′NIKOVA, *Sov. Phys.-Solid State* **2** (1961) 2428.
2. Y. YOKOMIZO and S. NOMURA, *J. Phys. Soc. Jpn.* **28**(suppl.) (1970) 150.
3. Y. YAMASHITA, *Am. Ceram. Soc. Bull.* **73** (1994) 74.
4. Y. MATSUO, H. SASAKI, S. HAYAKAWA, F. KANAMARU and M. KOIZUMI, *J. Am. Ceram. Soc.* **52** (1969) 516.
5. P. RAVINDRANATHAN, V. SRIKANTH, S. KOMARNENI and A. S. BHALLA, *Ferroelectrics* **188** (1996) 135.
6. J. WANG, D. WAN, J. XUE and W. B. NG, *J. Am. Ceram. Soc.* **82** (1999) 477.
7. T. R. SHROUT and A. HALLIYAL, *Am. Ceram. Soc. Bull.* **66** (1987) 704.
8. H. C. LING, M. F. YAN and W. W. RHODES, *Ferroelectrics* **89** (1989) 69.
9. W. F. SMITH, in "Principles of Materials Science and Engineering" (2nd ed.) (McGraw-Hill, Singapore, 1990) p. 37.
10. J.-S. KIM, N.-K. KIM and H. KIM, *J. Am. Ceram. Soc.* **86** (2003) (in printing).
11. B.-H. LEE, N.-K. KIM, J.-J. KIM and S.-H. CHO, *Ferroelectrics* **211** (1998) 233.
12. B.-H. LEE, N.-K. KIM and B.-O. PARK, *ibid* **227** (1999) 87.
13. S. L. SWARTZ and T. R. SHROUT, *Mater. Res. Bull.* **17** (1982) 1245.
14. S. L. SWARTZ, T. R. SHROUT, W. A. SCHULZE and L. E. CROSS, *J. Am. Ceram. Soc.* **67** (1984) 311.
15. M.-C. CHAE and N.-K. KIM, *Ferroelectrics* **209** (1998) 603.
16. B.-Y. AHN and N.-K. KIM, *J. Am. Ceram. Soc.* **83** (2000) 1720.
17. S. G. JUN and N. K. KIM, *J. Mater. Sci.* **35** (2000) 2093.
18. M.-C. CHAE, N.-K. KIM, J.-J. KIM and S.-H. CHO, *Ferroelectrics* **211** (1998) 25.
19. R. D. SHANNON, *Acta Cryst.* **A32** (1976) 751.
20. B.-Y. AHN and N.-K. KIM, *Mater. Res. Bull.* **35** (2000) 1677.
21. D.-H. SUH, N.-K. KIM and J.-H. KIM, *Mater. Lett.* **50** (2001) 6.
22. B.-Y. AHN and N.-K. KIM, *J. Mater. Sci.* **37** (2002) 4697.

Received 26 October 2001
and accepted 3 April 2003